

Article

The Potential of Chemically Recuperated Power Cycles in Markets with High Shares of Variable Renewables

Carlos Arnaiz del Pozo ^{1,*}, Ángel Jiménez Álvaro ^{1,*}, Schalk Cloete ²
and Jose Antonio García del Pozo Martín de Hijas ¹

¹ Departamento de Ingeniería Energética, Escuela Técnica Superior de Ingenieros Industriales, Universidad Politécnica de Madrid, Calle José Gutiérrez Abascal 2, 28006 Madrid, Spain

² Process Technology Department, SINTEF Industry, NO-7465 Trondheim, Norway; schalk.cloete@sintef.no

* Correspondence: cr.arnaiz@upm.es (C.A.d.P.); a.jimenez@upm.es (Á.J.Á.)

Abstract: Rising shares of variable wind and solar generation in decarbonized electricity systems motivate the development of novel power cycles employing unconventional fuels. Innovative designs must be highly flexible and profitable at low capacity factors, requiring a simple process layout and low capital costs. Fuel supply infrastructure represents a significant additional capital cost, which is often ignored in economic assessments of gas-fired power plants. When these capital costs are included, liquid fuels such as NH₃ or MeOH gain relevance despite their high production costs because they are cheap to store and distribute. In addition, chemically recuperated power cycle designs upgrade these fuels with waste heat from the gas turbine exhaust, avoiding a capital-intensive bottoming cycle while achieving high thermal efficiencies. This work presents an exergoeconomic benchmarking of different large-scale power plants and their fuel supply infrastructure. The results show that chemically recuperated cycles using MeOH become competitive relative to natural-gas-fired combined cycles with fuel storage in salt caverns at capacity factors below 32% if seven-day storage is required and plants are located 500 km from the fuel source. NH₃ can compete with H₂ at a higher capacity factor of 47% because of the high cost of storing H₂, while a CO₂ price of 140 EUR/ton is required for NH₃ to outperform MeOH as a fuel. In cases where salt cavern storage is unavailable, or the energy security of multi-week fuel storage is highly valued, liquid fuels present a clearly superior solution.

Keywords: energy vector; methanol; ammonia; techno-economic assessment; exergy; efficiency



Citation: Arnaiz del Pozo, C.; Jiménez Álvaro, Á.; Cloete, S.; García del Pozo Martín de Hijas, J.A. The Potential of Chemically Recuperated Power Cycles in Markets with High Shares of Variable Renewables. *Energies* **2023**, *16*, 7046. <https://doi.org/10.3390/en16207046>

Received: 30 August 2023
Revised: 4 October 2023
Accepted: 6 October 2023
Published: 11 October 2023



Copyright: © 2023 by the authors. Licensee MDPI, Basel, Switzerland. This article is an open access article distributed under the terms and conditions of the Creative Commons Attribution (CC BY) license (<https://creativecommons.org/licenses/by/4.0/>).

1. Introduction

The increasing penetration of renewable wind and solar in the power mix [1] to reduce greenhouse gas (GHG) emissions in the energy sector motivates the development of alternative power cycles that can adjust in a cost-competitive way to renewable intermittency. Long periods during which there is no renewable energy availability present an opportunity for novel thermal power plant designs, requiring a reduced capital expenditure to be economically attractive when operating under low capacity factors (CFs). Given the operating variability of the plants in such a scenario, gaseous fuels are advantaged over coal or nuclear, which present a lower degree of flexibility to respond to changes in demand and supply [2]. Despite this, substantial additional capital costs are incurred for the transmission and storage infrastructure needed to ensure a secure supply of fuel. Hydrogen (H₂) is the carbon-free energy vector that is postulated to enable a low-carbon economy [3] and offers the possibility of sector coupling, storage and end-use flexibility [4]. However, several issues have been highlighted regarding the transmission and storage of H₂ [5].

To overcome the technical and safety challenges associated with H₂, methanol (MeOH) and ammonia (NH₃) appear as emerging fuels in new power generation systems [6]. NH₃

presents itself as an attractive carbon-free candidate since it features a higher volumetric energy density and is easily liquefied at atmospheric pressure at around $-33\text{ }^{\circ}\text{C}$ [7]. On the other hand, MeOH is easily transported and stored as a liquid at ambient temperature, although it is a carbon-based molecule. A decrease in capital costs of gas-fired power plants designed for low operating hours implies a thermal efficiency reduction. One avenue to mitigate this efficiency loss while avoiding the costly and bulky bottoming steam cycle of traditional combined cycles (CCs) is the use of chemically recuperated gas turbines. Originally, this power cycle scheme was conceived for natural gas reforming employing gas turbine exhaust heat to attain efficiencies above those of a conventional steam-injected gas turbine (STIG) [8]. Pashchenko et al. [9] present an assessment of the optimal operating conditions for a methane-fired gas turbine using reforming with exhaust heat. However, using NH_3 or MeOH as alternative fuels allows the further enhancement of this innovative power cycle by effectively integrating the exhaust heat of the gas turbine to chemically upgrade these fuels, due to the endothermic nature of the decomposition/reforming reactions, which take place at lower temperatures than natural gas reforming, therefore achieving higher conversion rates. This characteristic makes MeOH well positioned as a transportable energy carrier for fuel cell applications [10,11]. NH_3 has also been investigated, showing promising results in high-temperature solid oxide fuel cells [12]. Nevertheless, despite the higher thermal conversion to electricity compared to thermal power plants, the scale of fuel cell technology is currently in the range of a few MW and presents a high specific capital investment.

Several studies evaluate the techno-economic potential of these fuels in conventional combined cycles or alternative set-ups involving chemical recuperation for large power generation capacities. For NH_3 , Cesaro et al. [13] carried out a techno-economic study of dispatchable power generation systems fueled by “green” NH_3 , namely NH_3 which is synthesized with electrolyzers for H_2 production using renewable wind and solar as primary energy; they highlight that at a projected cost of 400 EUR/ton, combined cycle power plants with NH_3 crackers operating at a 25% capacity factor can compete with other avenues of dispatchable, low-carbon technologies. Pashchenko et al. [14] evaluated a chemically recuperated gas turbine using NH_3 over a wide range of operating conditions, pointing out that additional recuperation systems such as steam injection show great potential to further improve efficiency. In this line, Shen et al. [15] investigated the design of NH_3 thermal decomposition integration in a power cycle, revealing that an efficiency 1.7%-points lower than that of a natural-gas-fired combined cycle can be reached through decomposition and steam injection. With regard to MeOH, Pashchenko [16] revealed that a combined cycle with MeOH decomposition using low-grade heat achieves 5.2%-points higher efficiency than a MeOH combined cycle with direct combustion of the fuel. Tola et al. [17] evaluated the use of chemically recuperated power cycles using MeOH from renewable sources, employing CO_2 capture after fuel combustion to recycle the CO_2 molecule for hydrogenation and subsequent MeOH synthesis; despite a low power-to-power efficiency of 23%, the system can effectively store excess renewable power. A performance assessment dealing with the integration of low-temperature solar energy for MeOH decomposition in a humid air turbine (HAT) was conducted by Zhao et al. [18], underlining that an exergy efficiency increase of 5.5%-points can be achieved relative to the conventional HAT cycle. Solar-assisted chemical upgrading of MeOH for combined cooling, heat and power generation was the topic of a study by Liu et al. [19], revealing that the combination of solar-thermal chemical conversion and recuperation with energy storage can achieve an overall energy efficiency of 80.55%. However, it should be mentioned that additional capital costs for integrating CCS and/or solar collectors may soon prove uneconomical for power generation plants intended to operate at low capacity factors and employing costly synthetic fuels such as MeOH.

The objective of this work is to carry out an exergoeconomic evaluation of chemically recuperated cycles for large-scale power generation employing liquid fuels such as methanol (MeOH) and ammonia (NH_3) relative to gaseous fuels (natural gas and H_2) used

in conventional combined cycles. The primary novelty relative to the existing literature is that fuel storage and transmission costs are considered to provide a comprehensive perspective of different fuels in future electricity systems where thermal power plants (and their fuel supply infrastructure) must operate at low utilization rates. An additional novelty is the methodologically consistent techno-economic assessment of thermal power cycles where the different fuel costs are determined based on the same baseline cost of natural gas energy input, employing previous techno-economic assessments developed by the authors [20–22].

In the following sections, the modeling assumptions for the different power cycles are provided and the plant key performance indicators are defined, while the cost estimation methodology for the power units as well as the storage and transmission infrastructure is described. Subsequently, the results of the assessment in terms of energy, environmental, exergy and economic metrics are presented. Appropriate sensitivity studies are conducted for key economic assumptions. Finally, the main findings of the study are summarized and discussed.

2. Methodology

2.1. Power Cycle Modeling

The models were created using Unisim Design R481 employing Peng–Robinson for property estimation of gaseous mixtures and ASME steam tables for water and steam. Firstly, a combined cycle (CC) model with either natural gas or hydrogen as fuel was developed. Secondly, post-combustion CO₂ capture (PCC) was integrated in the natural-gas-fired case based on [23]. Using the calibrated performance of the NGCC [24], H₂CC and chemically recuperated power cycle models using MeOH and NH₃ were developed.

The CC consists of an H-class turbine and a heat recovery steam generator (HSRG) with three pressure levels and reheat, as depicted in Figure 1. While the CC scheme is designed for maximum efficiency, chemically recuperated power cycles with air recuperator and intercooler (ChRGT) and steam injection (ChSTIG) trade some efficiency for a reduction in capital costs to make them more attractive for operation at low CFs. Instead of the costly bottoming cycle present the CC configuration, ChRGT introduces an intercooler in the H-class turbine compression step to reduce compression power and a heat exchange recuperator to preheat the inlet air of the combustor to fully utilize the exhaust heat from the gas turbine, as shown in Figure 2. Due to the lower air temperature after the second compression stage, cooling flow requirements for this configuration are reduced. On the other hand, in the ChSTIG cycle, besides fuel upgrading in the heat recovery unit, water is pumped and mixed with the fuel, as shown in Figure 3, to reach a close temperature approach in the exchanger where it is vaporized and subsequently expanded across the turbine after the combustor. As a result, air is displaced from the compressor suction (to keep a constant turbine volumetric outlet), and therefore, compression duty is reduced.

The blade cooling flow parameters and component efficiencies for the natural-gas-fired case were calibrated using the GS code from Politecnico di Milano [25–27] for advanced gas turbine models similarly to previous works [24,28], using a simplified lumped cooling flow model for rotor and stator blades based on Jonsson et al. [29]. The technological developments required to operate the gas turbine at the nominal pressure ratio and combustor outlet temperature (COT) as for the natural-gas-fired case are assumed to simplify the evaluation when employing the other fuels. The gas turbine size was kept constant between the cases by designing each cycle with the same volumetric outlet flow rate from the turbine as for the natural-gas-fired case. The results of the calibration and main modeling assumptions for the combined cycle are provided in Table 1.

On the other hand, the modeling assumptions employed for the bottoming cycle, consisting of a heat recovery steam generator (HSRG) with three pressure levels (once-through high pressure boiler) and intermediate reheat, a steam turbine and a condenser system are presented in Table 2.

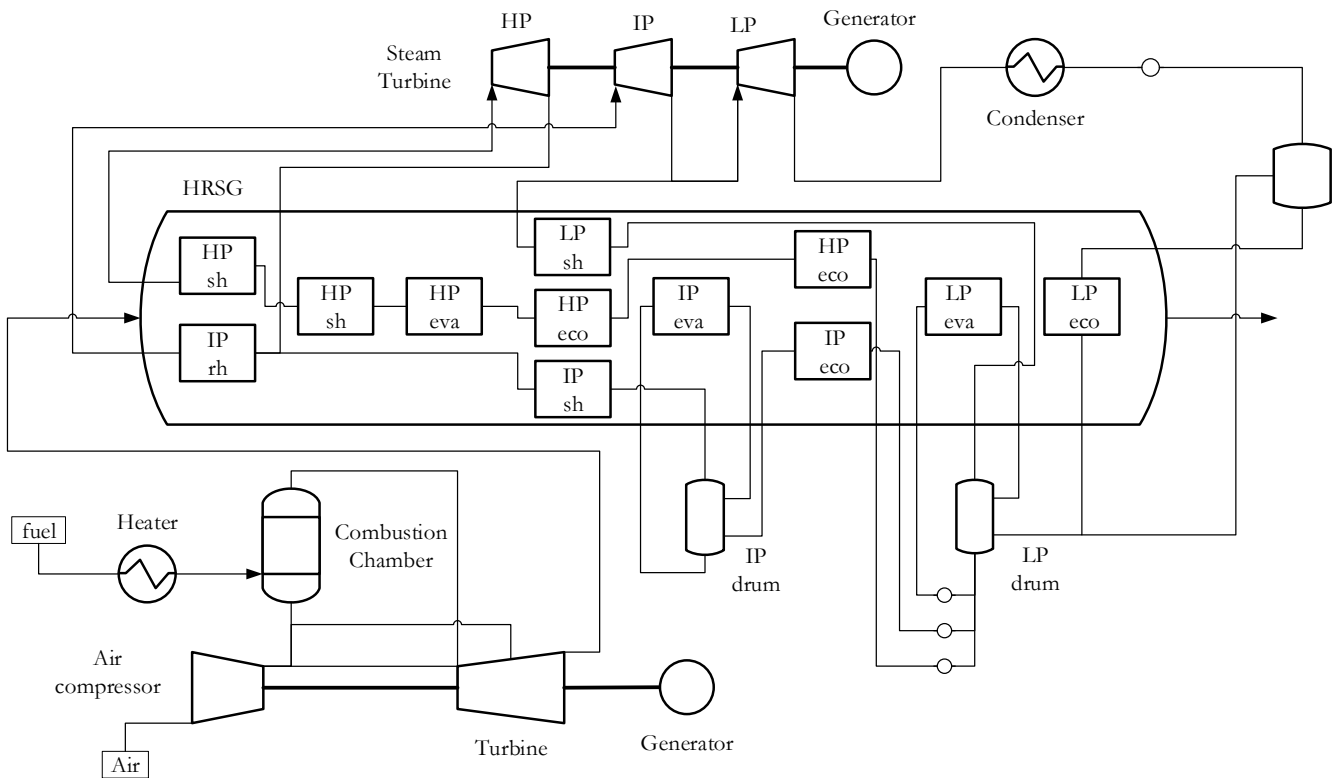


Figure 1. Schematic of the modeled combined cycle (CC).

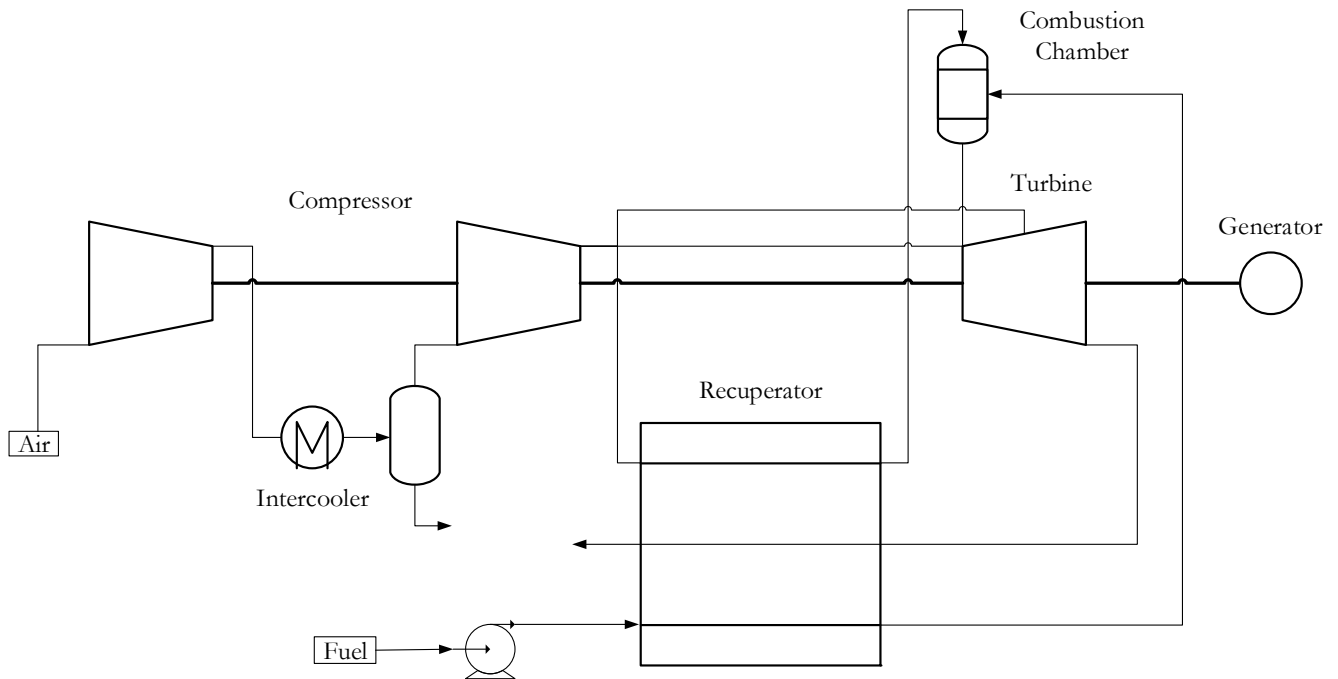


Figure 2. Schematic of the modeled chemically recuperated gas turbine cycle with air recuperator and intercooler (ChRGT).

In the ChRGT power cycles, the temperature approach considered in the hot end of the recuperator was 30 °C, whereas the design pinch point in the cold end was 10 °C, which are typical values assumed for gas–gas and gas–boiling fluid heat exchange [28]. Chemical upgrading through the conversion of MeOH and NH₃ was assumed to proceed with an approach to equilibrium of 10 °C. More detailed modeling considering decomposition

and reforming kinetics for MeOH [30] and NH_3 [31] revealed that the chemical reaction is greatly favored given the low operating pressures, leading to small reaction volumes relative to the area required for heat transfer to the tube, which is the limiting step because near-atmospheric pressure is encountered for the hot-side gases, leading to low heat transfer coefficients. Equilibrium conversion is favored at the temperatures present in the exhaust and at low pressures. A supply pressure of 35 bar was assumed after the liquid fuel pump to enable a substantial overpressure for fuel injection in the combustion chamber [32].

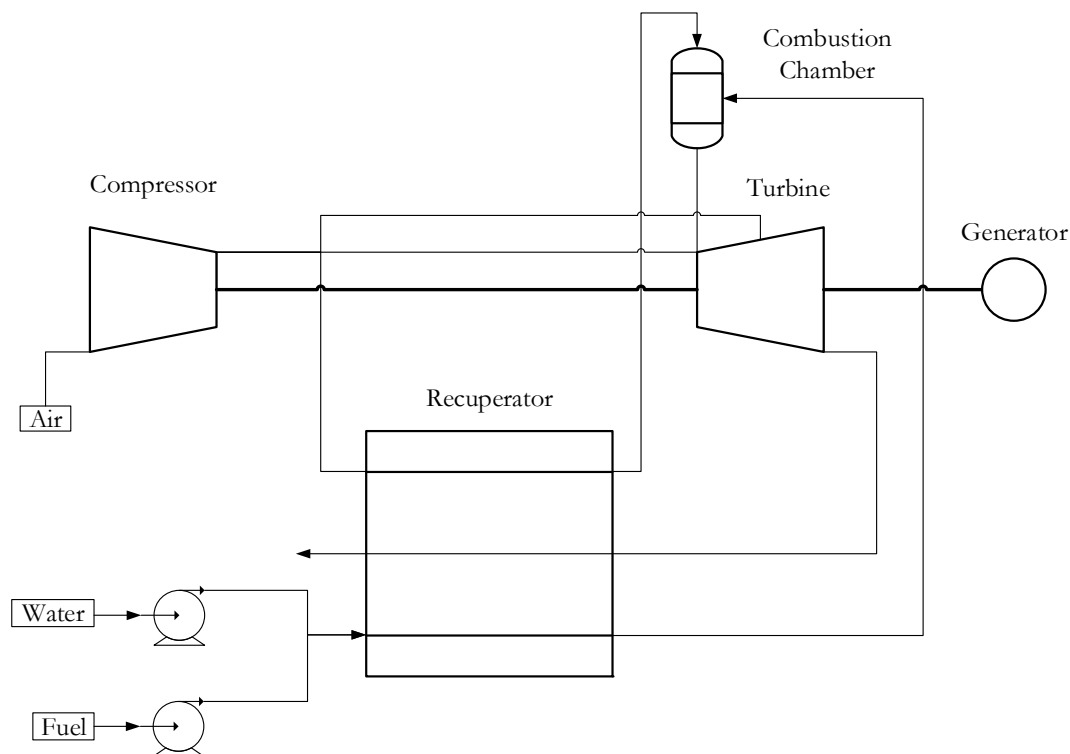


Figure 3. Schematic of the modeled chemically recuperated gas turbine cycle with steam injection (ChSTIG).

Table 1. Gas turbine calibrated efficiencies and parameters for air at 15 °C and relative humidity of 60%.

Item	Value	Unit
Compressor polytropic efficiency	92.86	%
Compressor leakage	0.4	%
Turbine polytropic efficiency (1st stage, remaining)	90.0/89.0	%
Combustor outlet temperature	1651	°C
Combustor pressure drop	3	%
Combustor heat loss	0.4	%LHV
Mechanical efficiency	99.86	%
Generator efficiency	98.7	%
Blade temperature (1st stator, 1st rotor, remaining)	900/875/850	°C

In the present study, it is assumed that catalysts can be effectively located in the heat exchange process such that the chemical conversion is achieved. For MeOH, the ChRGT case only considers decomposition through Equation (1). In the ChSTIG cycle, reforming with a lower endothermicity occurs through a Cu-based catalyst (Equation (2)). Finally,

NH_3 decomposition is modeled according to Equation (3), under the assumption that a Ni-based catalyst can cope with a large water fraction in the ChSTIG case.

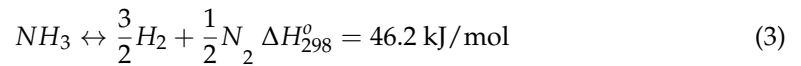
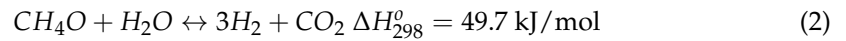
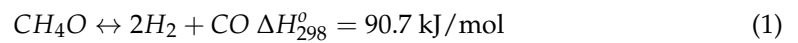


Table 2. Bottoming cycle modeling assumptions [28].

Item	Value	Unit
HP/IP/LP evaporator temperature approach	-/9/9	%
HP/IP/LP evaporator temperature pinch	9/10/10	%
HP/IP/LP evaporator pressure	185/43/5	%
Boiler feedwater temperature	60	°C
Maximum steam temperature	600	°C
Condenser pressure	0.04	bar
HP/IP/LP steam turbine adiabatic efficiency	98.3/92.0/87.7	%
Mechanical efficiency	99.6	%
Generator efficiency	98.7	%

An important simplification of the model is that irrespective of the fuel, NO_x emissions are assumed to remain within regulatory constraints. It should be noted that NH₃ combustion poses greater concerns regarding NO_x formation, although a high fuel decomposition level and steam injection mitigate this issue [15]. Alongside this, sufficient development is assumed in line with recent progress in combustion technology to cope with 100% H₂ fuel in gas turbines [33].

2.2. Plant Key Performance Indicators

A basic outline of the plant performance indicators other than economic metrics determined for the different power cycles is provided in this section. Firstly, the thermal efficiency of the plant is calculated according to Equation (4) as the ratio between the net power output of the plant and the fuel heat input, on a lower heating value basis.

$$\eta_{El} = \frac{\dot{W}_{net}}{\dot{m}_{fuel} LHV_{fuel}} \quad (4)$$

Environmental metrics of the power generation scheme are reflected in terms of specific CO₂ emissions, in those plants which employ a carbonaceous fuel, as shown in Equation (5). CO₂ emissions that arise from fuel manufacturing are accounted for as a CO₂ tax in the fuel cost:

$$E_{CO_2} = \frac{\dot{m}_{CO_2}}{\dot{W}_{net}} \quad (5)$$

The exergy balance to a system j with i mass stream inlets and outlets reflected in Equation (6) is applied to each of the power cycle components assuming stationary operation, with the exergy flows calculated according to [34], considering the physical (due to pressure and temperature differences relative to the environment) and chemical (due to composition differences with the environment) contributions, as shown in Equation (7):

$$\frac{dB_j}{dt} = \int d\dot{Q}_j \left(1 - \frac{T_0}{T} \right) - \left(\dot{W}_j - P_0 \frac{dV_j}{dt} \right) - \dot{I}_j + \sum_i e_{i,j} \dot{m}_{i,j} \quad (6)$$

$$e_i = e_{ph} + e_{Ch} \quad (7)$$

The first term of Equation (6) indicates the content of heat which is interchangeable with work and depends on the Carnot factor, i.e., the temperature at which heat is exchanged and the ambient temperature. The second term is the useful content of work, in which expansion against the ambient is subtracted (since we are dealing with rigid systems with no change in volume with time, this becomes zero). I is defined as the exergy destruction that takes place in system j , representing the energy that is lost due to the irreversible nature of the process that occurs in the system. Thus, the irreversibility sources of the power cycle can be quantified. Finally, the summation term indicates the exergy that is added or removed from the system in the form of mass exchange. The rational efficiency of the plants is defined according to Equation (8):

$$\zeta = \frac{\dot{W}_{net}}{\dot{E}_{fuel}} \quad (8)$$

2.3. Fuel Transmission and Storage

To account for transmission and storage costs between the different fuels, two scenarios (Sc1, Sc2) for NG and H₂ fuels are considered, while only one is considered for NH₃ and MeOH (Sc1), as shown in Figure 4:

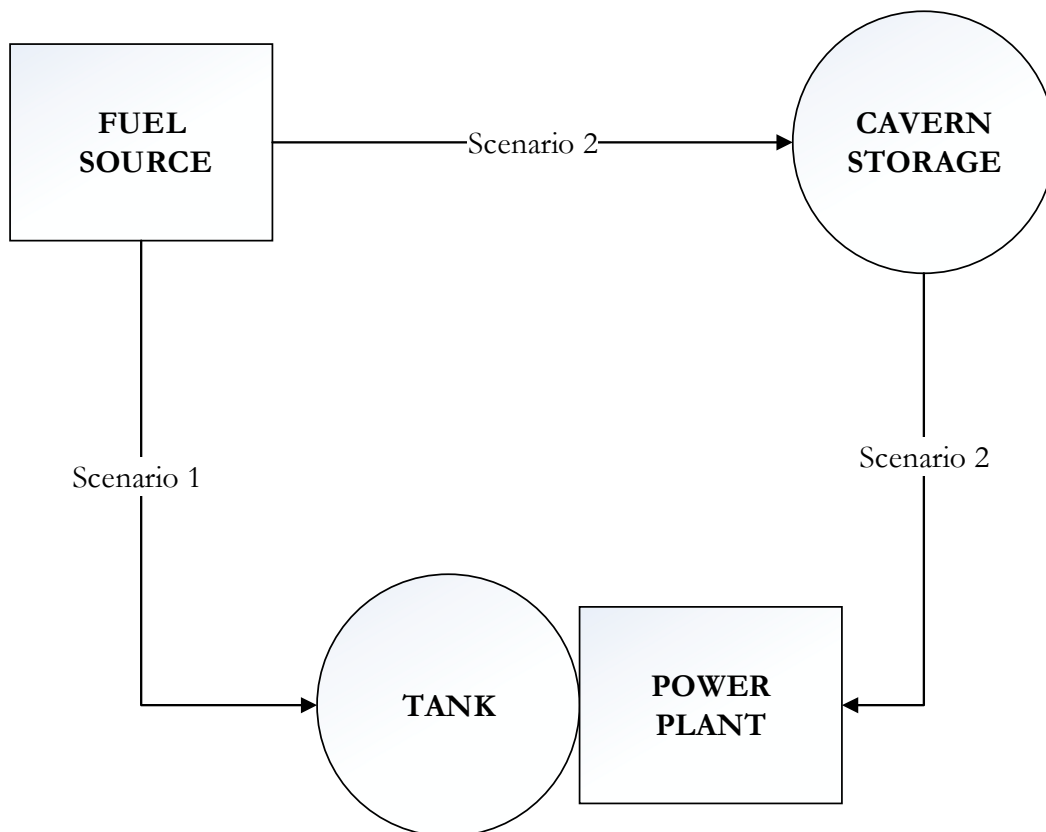


Figure 4. Schematic of the two transmission and storage scenarios considered.

Sc1: Steady-state pipeline supply and on-site tank storage;

Sc2: On-demand pipeline imports from distant underground cavern storage.

For natural gas and hydrogen, storage in an underground cavern is approximately an order of magnitude less capital-intensive than on-site storage in tanks. However, if the cavern is located far away from the fuel source or the power plant, the saving in storage costs is offset by additional expenses for pipeline transmission [35]. To enable a consistent

comparison between Sc1 and Sc2, a cavern/tank pipeline ratio is defined to represent the additional pipeline length in Sc2 relative to that in Sc1, which is required to reach the cavern. For the base case analysis, the ratio is set to 2, meaning that the pipeline in Sc2 is twice as long as in Sc1. An alternative scenario that is not envisioned in the present study would be the use of a natural gas liquefaction peak-shaving plant for the storage of this fuel. However, the effect of such a storage means can be easily assessed in the primary energy cost sensitivity analysis, as this extra scope would result in a relative increase in fuel cost delivered to the power cycle. As explained later, transmission and storage costs are accounted as a capital expenditure item in the assessment because the purpose is to convey the cost of the whole value chain for each fuel.

The transmission and storage costs employed in the economic evaluation are provided in Table 3 for each fuel. An inflation factor of 50% with respect to the values reported in [35] was assumed for the pipeline costs, as the lowest of two cost bases differing by a factor of three was taken in that reference. Additionally, double the cavern storage cost for H₂ was considered, as typically only half of the cavern storage capacity can be effectively utilized [36]. The storage cost of natural gas was estimated as a third of that of H₂ since the former presents a 3× higher volumetric energy density. Finally, an almost negligible storage cost for MeOH (which is a liquid at ambient temperature) was assumed as half of the storage cost for NH₃.

Table 3. Summary of assumed storage and transmission costs [35,37,38].

Fuel	Tank Storage (USD/kWh)	Cavern Storage (USD/kWh)	Pipeline Scale (GW)	Pipeline Cost (MUSD/km)
H ₂	15.6	2.1	8.36	1.29
NG	5.2	0.7	17.39	1.57
NH ₃	0.2		27.41	1.89
MeOH	0.1		37.44	1.78

The cost of storage was assumed to scale linearly with the specific costs given in Table 3, given that tank storage would be scaled modularly and cavern storage is to a large degree predetermined by the geological formation available. However, pipeline costs are subjected to a scaling exponent (n) of 0.5 from the baseline scale (S_0) and cost (C_0) for the 36-inch pipeline represented in Table 3, according to Equation (9).

$$C = C_0 \left(\frac{S}{S_0} \right)^n \quad (9)$$

The effect of this scaling is that the pipeline costs of the different fuels differ less than might be expected for the scale of the power plants investigated in this study (~1 GW of fuel input). For example, even though the specific cost of an NG pipeline is only about half that of an H₂ pipeline if the pipeline diameter is kept constant (because the same size of a pipeline can deliver twice as much NG as H₂ due to the 3× higher volumetric energy density of natural gas partially offset by its higher viscosity requiring lower pipe velocities), the NG pipeline would need to be scaled down more to reach the required scale, experiencing lower economies of scale ($n = 0.5$).

For Sc2, the pipeline was sized to facilitate the maximum generating capacity of the power plant. On the other hand, the pipeline supplying Sc1 was undersized, relying on the on-site fuel storage as a buffer between a steady inflow of fuel and intermittent outflows to feed the power plant when required. However, the pipeline was sized larger than the assumed CF of the plant to allow for some longer-term variations in plant load (caused by, for example, seasonal variations in wind and solar output). Specifically, the pipeline was sized halfway between the plant CF and 100% of the maximum generating capacity. For example, if the assumed CF was 40%, the pipeline was sized to $(40\% + 100\%)/2 = 70\%$ of the maximum fuel input.

2.4. Economic Assessment

Economic evaluations were developed with the Standardized Economic Assessment (SEA) tool created by the authors [39]. A dedicated spreadsheet for each case is available for download online [40]. To ensure consistency in the cost of different fuels, prior techno-economic assessments of NG conversion to different fuels with integrated CO₂ capture [20,21] are deployed with a base NG cost of 6.5 EUR/GJ and a CO₂ tax of 100 EUR/ton (given that not 100% of the CO₂ which is generated in the synthesis process is ultimately captured), yielding the fuel production costs shown in Figure 5. As shown, H₂ and MeOH are more than twice as expensive as the NG from which they are produced, while NH₃ is over triple the cost. Advanced configurations for producing these fuels could reduce the cost of hydrogen and NH₃ by about 14% [20] and MeOH by about 6% [21]; therefore, a dedicated sensitivity of the fuel premium cost (relative to the natural gas primary energy cost) is determined. Therefore, Figure 5 shows factory gate costs before additional distribution costs required for reliable fuel supply to power plants. Thus, fuel transmission and storage costs are lumped into the capital costs of the power generation systems described in the preceding section.

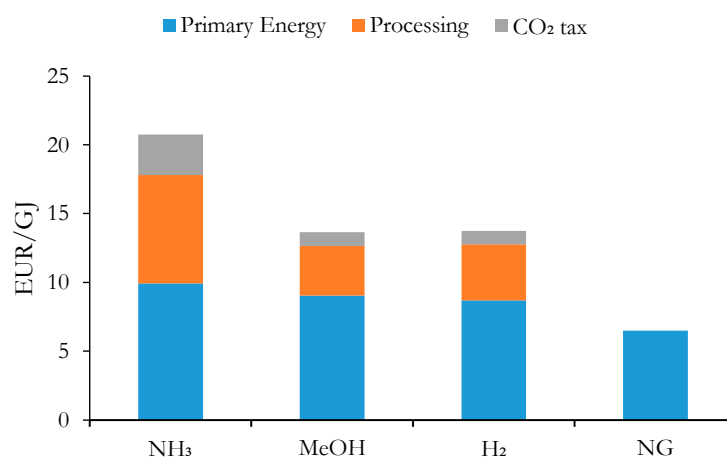


Figure 5. Fuel cost breakdown, assuming that NH₃, MeOH and H₂ are produced from natural gas using currently available technology as assessed in prior works [20,21].

The assessment was completed in euros for the year 2020 and for a Western European construction site under the base-case assumptions outlined in Table 4. A process contingency of 10% was employed for the power plant components to account for flexible power cycle operation. For the chemical recuperator, the cost–capacity correlation based on an HSRG from [23] was used, given that heat transfer is the dominant effect and will determine the size of the unit. The evaluation assumed a construction period of 2 years for combined cycle configurations (due to the larger scope required for the bottoming cycle and cooling tower) and 1 year for the power cycles employing one gas turbine.

CO₂ transmission and storage costs for the post-combustion capture plant were estimated assuming a total cost of 20 EUR/ton for a plant operating at an 85% capacity factor, in which fixed capital costs are 15 EUR/ton and variable operating costs are 5 EUR/ton [41,42]. This methodology enables a more realistic prediction of costs associated with this item when the plant operates at lower capacity factors compared to evaluations assuming 20 EUR/ton as a variable cost, which would present an optimistic estimate.

Finally, the levelized cost of electricity (LCOE) is determined as the selling price that yields a net present value (NPV) of zero (Equation (10)). The NPV results from summing the discounted annual cash flows in Equation (11) throughout the plant’s operational lifetime.

$$NPV = \sum_{t=0}^n \frac{ACF_t}{(1+i)^t} \quad (10)$$

$$ACF_t = CF \cdot (LCOE \cdot P_{El.} - C_{VOM}) - C_{Capital} - C_{FOM} \quad (11)$$

Table 4. Economic assumptions.

Capital Estimation Methodology		
	Bare Erected Cost (BEC)	SEA Tool Estimate
Engineering procurement and construction (EPC)		10% BEC
Process contingency (PC)		0–10% BEC
Project contingency (PT)		20% (BEC + EPC + PC)
Owner's costs (OC)		15% (BEC + EPC + PT + PC)
Total overnight costs (TOC)		BEC + EPC + PC + PT + OC
Transmission and storage assumptions		
Sc1 pipeline length	500	km
Cavern/tank pipeline ratio	2	-
Storage volume	7	Days at full capacity
Operating and maintenance costs		
	Fixed	
Maintenance	2.5	%TOC
Insurance	1	%TOC
Labor	60,000	EUR/y-p
Operators	2	persons
	Variable	
NG fuel	6.5	EUR/GJ
CO ₂ tax	100	EUR/ton
Process water	6	EUR/ton
Make-up water	0.35	EUR/ton
Cash flow analysis assumptions		
1st year CF	31	%
Remaining years	40	%
Discount rate	8	%
Construction period	1/2	years
Plant Lifetime	25	years

3. Results and Discussion

The results are provided in four sections. First, the energy and environmental performance of the cases is briefly presented. The exergy breakdown and exergy flow diagrams are then discussed. The outcomes of the economic assessment are subsequently considered. Finally, sensitivity studies for key economic assumptions are portrayed.

3.1. Energy and Environmental

The thermal efficiency and CO₂ footprint of the power plants for the different cycles and fuels are provided in Table 5.

Table 5. Energy and environmental results.

Fuel		NG		H ₂	MeOH		NH ₃	
Power Cycle		CC	PCC	CC	ChRecGT	ChSTIG	ChRecGT	ChSTIG
Heat Input	MW _{th}	1196.5	1197.1	1184.6	995.6	966.7	1075.6	965.0
Gross Power	MW _{th}	753.3	688.8	760.6	636.7	597.8	660.0	599.6
Auxiliaries	MW _{El}	9.9	41.1	10.3	2.5	3.1	2.6	3.0
\dot{W}_{net}	MW _{El}	743.4	647.7	750.3	634.2	594.7	657.4	596.7
η	%	62.1%	54.1%	63.3%	63.7%	61.5%	61.1%	61.8%
E_{CO_2}	kgCO ₂ /MWh	330.1	35.2	0.0	389.8	403.6	0.0	0.0

The emissions intensity of the different plants is simply related to the fuel carbon content and the plant efficiency. The PCC case was modeled to achieve a 90% capture rate, resulting in an 8.0%-points energy penalty, a consistent result with previous assessments [24]. The efficiency of the H₂CC outperformed the natural-gas-fired case by 1.2%-points, resulting from the larger enthalpy drop due to the higher concentration of water in the exhaust gases [27]. As discussed, the power cycles are sized to reach the same volumetric outlet flow in the expansion turbine at a fixed COT of 1651 °C. Since the liquid fuels are thermally upgraded in the power cycle recuperator, the resulting heating value input in the combustor is larger than that in the fuel input system. Overall, this leads to a comparatively lower heat input to the plant (given that the volumetric flow across the turbine is constrained) and, alongside this, a relatively lower net power output compared to the combined cycle configurations. In the cases with chemical decomposition, heat from the exhaust gases is recycled for fuel upgrading (and steam injection displacing air from the compressor and reducing compressor duty), whereas in the conventional power scheme, a bottoming cycle further extracts power from that heat in a steam turbine.

It is noteworthy to evaluate the gain achieved by chemical recuperation relative to fuel switching, i.e., the use of direct combustion of liquid fuels after pressurization and vaporization in the combustion chamber of a combined cycle or a recuperated gas turbine (RGT), instead of natural gas or H₂. The modeling and techno-economic assessment of these power schemes was addressed in a prior technical report [43]. The net efficiency trade-offs between chemically recuperated power concepts and the CC and RGT power schemes with direct fuel combustion are provided in Figure 6, showing results for RGT with and without fuel upgrading, the CC and the chemically upgraded STIG cycle. In the cycles with fuel pre-conversion, the efficiency gap with respect to the CC is substantially diminished relative to the RGT case with direct combustion of MeOH and NH₃.

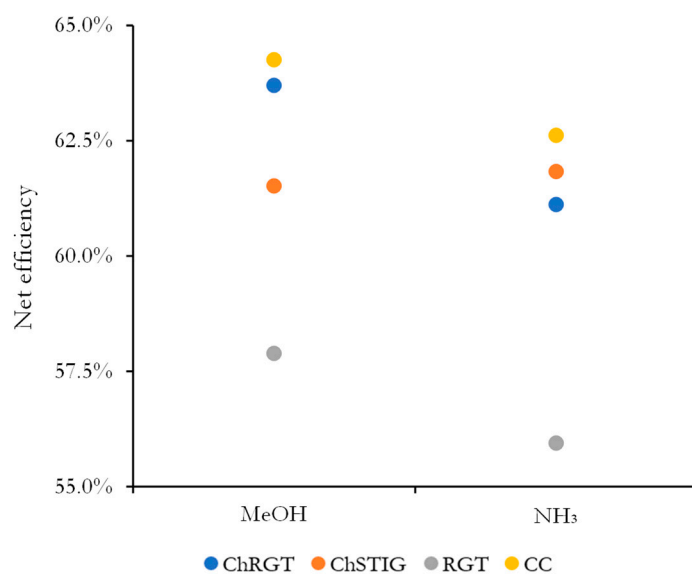


Figure 6. Net efficiency for different power cycles with NH₃ and MeOH as fuels.

The MeOH ChRGT presents a significant efficiency advantage over the ChSTIG counterpart because the decomposition reaction (Equation (1)) considered reveals a higher endothermicity than reforming (Equation (2)), allowing for a greater enhancement of the fuel heating value prior to the combustion chamber relative to the other cases. For NH₃, on the contrary, the ChSTIG configuration results in slightly higher thermal performance because water injection enables a cold section temperature pinch, maximizing heat recovery from the exhaust gases, as well as displacing a significant amount of air from the compressor to reach the same volumetric outlet in the turbine. This has a larger effect on performance compared to the intercooled compression arrangement of the ChRGT.

3.2. Exergy

The exergy destruction breakdown and the exergy efficiency (useful effect) for each power cycle are provided in Figure 7. The Miscellaneous section includes electromechanical losses of the turbomachinery, while the exergy loss represents the useful energy contained in the exhaust gases after heat recovery and, for the PCC case, the exergy of the captured CO₂ stream. Notably, in this case, greater exergy destruction takes place as a result of the added scope required to treat the exhaust gas stream for CO₂ removal. However, throughout all cases, the results convey that the largest source of irreversibility is found in the combustion chamber of the gas turbine, where the fuel is degraded to combustion products. The highest exergy efficiency is found for the H₂ combined cycle, which results from a chemical exergy for this substance closest to the LHV, relative to the more complex molecules. This can be explained due to the lower irreversibility which translates into a lower Gibbs free energy of combustion for H₂ compared to other fuels.

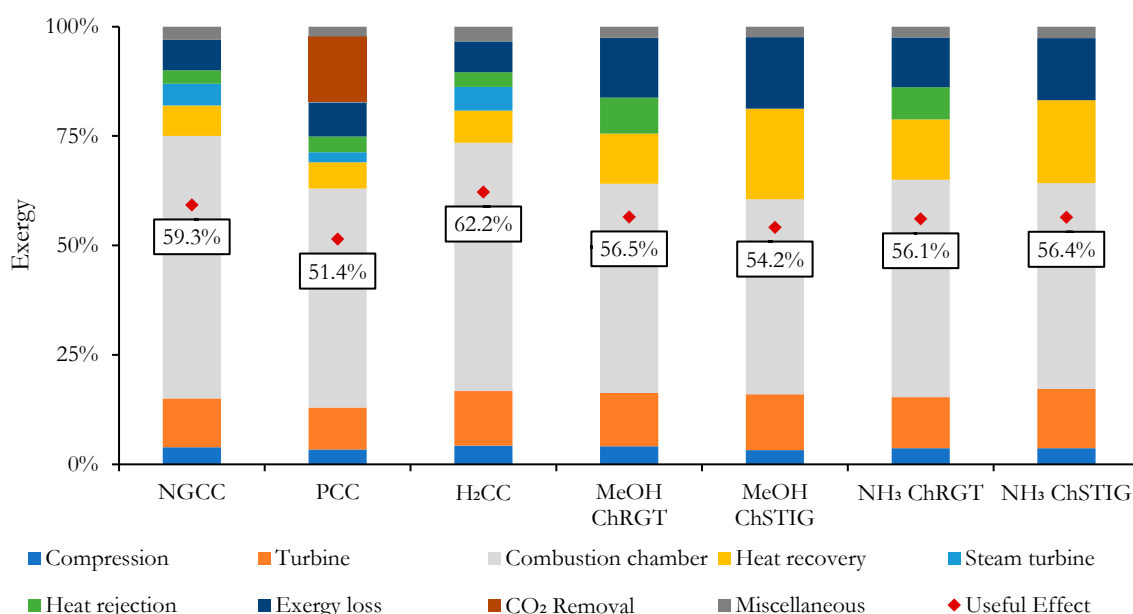


Figure 7. Exergy breakdown for the different power cycle configurations.

Interestingly, the losses corresponding to the expansion step (turbine) are comparatively greater than those of the compression path, given the mixing of cooling flows and the higher temperatures encountered in the former process, which lead to larger losses. Notably, the ChRGT schemes present greater exergy destruction in the heat rejection section due to the compressor intercoolers, where heat is rejected from high temperatures relative to the condenser, operating at close to ambient temperature, in the steam cycle of the CC configurations. The ChSTIG power cycles do not present a heat rejection unit; however, losses in the heat recovery section are substantially more due to the larger heat transfer taking place due to water evaporation, relative to the air recuperator in the ChRGT. Furthermore, the heat recovery section also reflects the losses associated with the chemical decomposition or reforming reaction taking place, which are the lowest for MeOH decomposition (Equation (1)) and greatest for MeOH reforming (Equation (2)). This explains the comparatively greater losses for ChSTIG in this section for MeOH fuel relative to NH₃. On the other hand, exergy losses in the ChSTIG are also greater because steam is lost in the exhaust gas stream, despite achieving lower exhaust outlet temperatures attained by water injection.

The exergy flow diagrams are illustrative of the exergy exchange between components of the power cycle. Such diagrams are shown for the NGCC case in Figure 8, the MeOH ChRGT case in Figure 9 and the NH₃ ChSTIG case in Figure 10, in order to reflect the most distinctive power cycle designs. It is noteworthy to realize that the exergy of the fuel inlet

to the combustion chamber for the chemically recuperated cycles is increased as a result of the thermal conversion taking place in the heat recovery unit, relative to the original exergy input of the fuel. For these diagrams, the heat recovery section is decomposed into sections of heat exchange and the chemical reaction taking place.

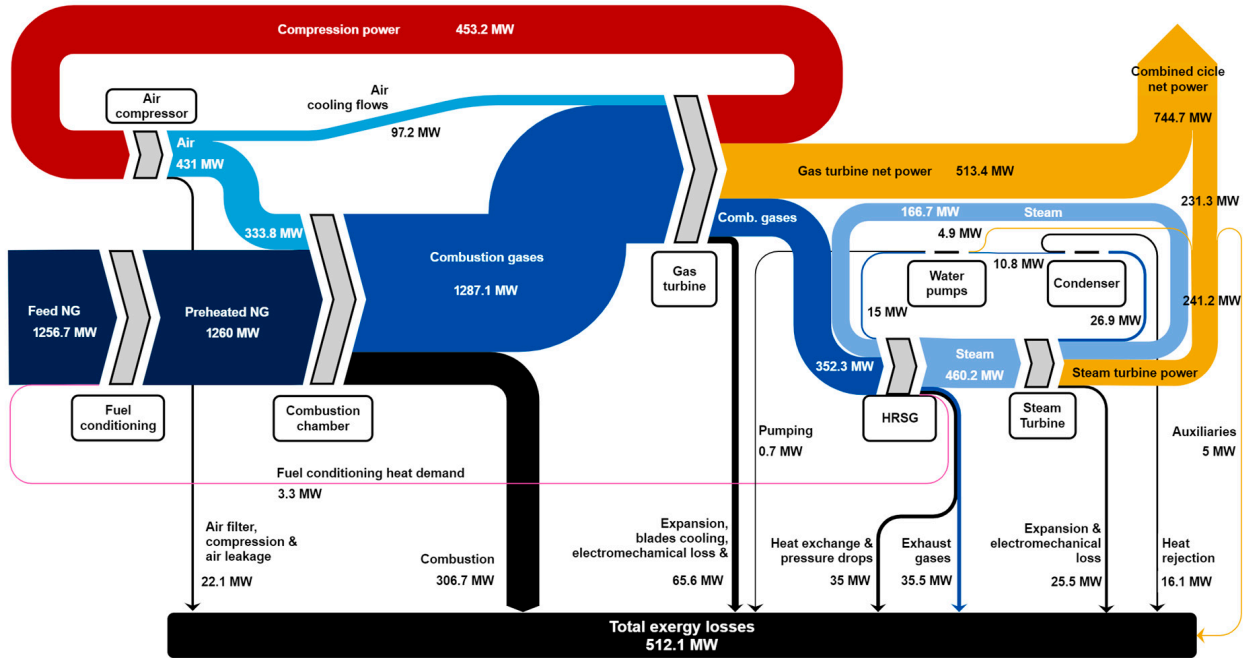


Figure 8. Exergy flow diagram of the NGCC case.

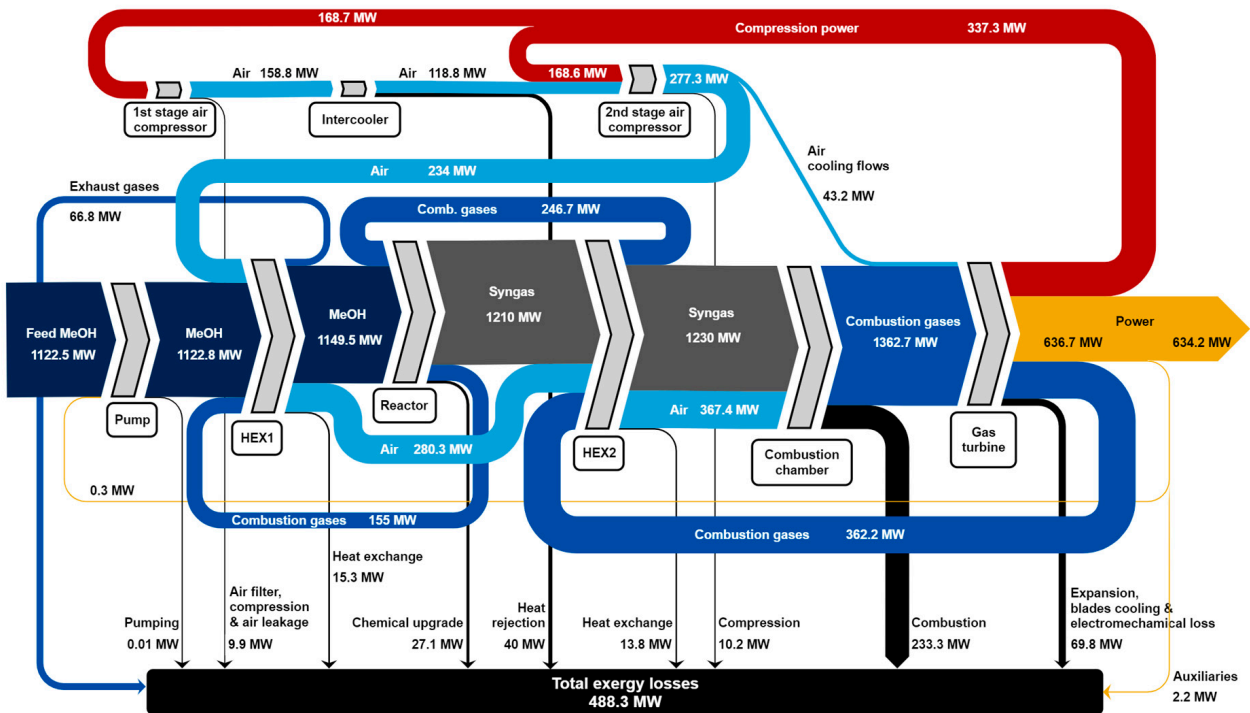


Figure 9. Exergy flow diagram of the MeOH ChRGT case.

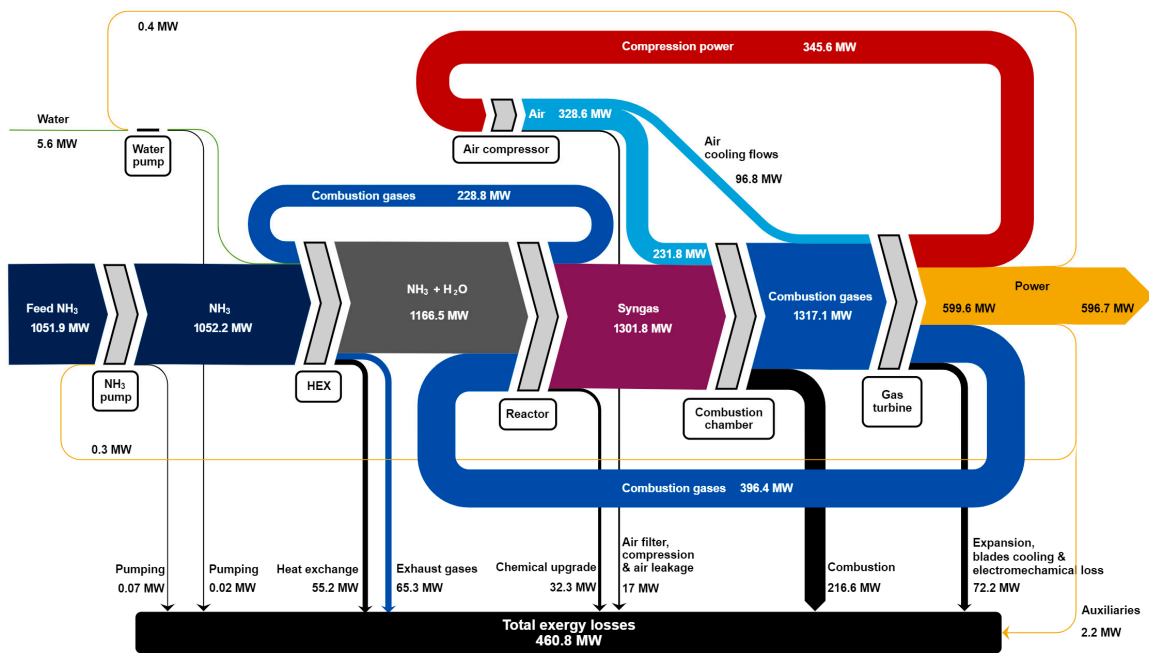


Figure 10. Exergy flow diagram of the NH₃ ChSTIG case.

3.3. Economic

The specific TOC is shown in Figure 11, with the main difference being the storage and transmission costs between the gaseous (NG and H₂) and liquid (MeOH and NH₃) fuels. The pipeline costs for the gaseous fuels are much larger than those for the liquid fuels due to several factors: (1) the pipeline length in Sc2 is assumed to be twice that of Sc1 to reach the cavern storage facilities, (2) the pipeline in Sc1 can be undersized due to the on-site fuel storage buffer, and (3) the specific costs of transporting liquid fuels are somewhat lower than those for transporting gaseous fuels. On-site storage costs for the liquid fuels are almost negligible, while cavern storage of the gaseous fuels still amounts to a considerable cost, especially for hydrogen (due to its 3× lower energy density compared to NG).

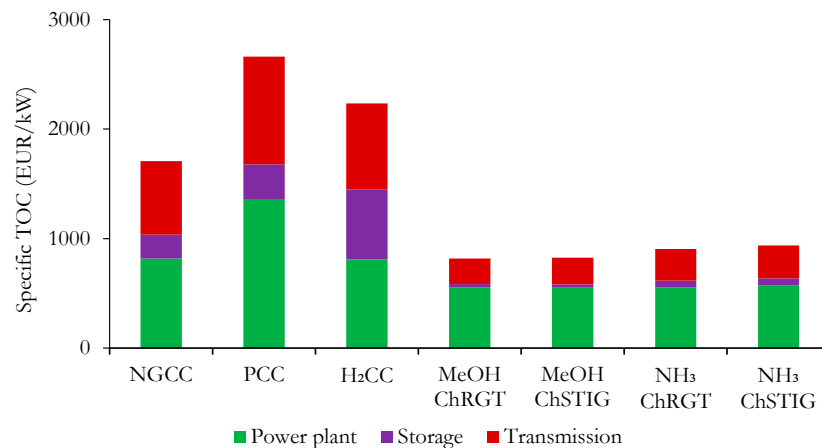


Figure 11. Specific total overnight cost for the different configurations using Sc2 for NG and H₂ and Sc1 for MeOH and NH₃. Transmission pipeline lengths are 1000 km for Sc2 and 500 km for Sc1 and storage is sized to 7 days at full capacity.

An important point to reflect is the degree to which chemical upgrading of the fuel contributes to reducing the cost of power generation using more valuable fuels such as ammonia or methanol as opposed to a conventional combined cycle or a recuperated gas turbine scheme where no pre-conversion (upgrading) of the fuel takes place. Such

comparison in terms of LCOE is provided in Figure 12 for capacity factors of 20% and 40%, using a CC and RGT (without chemical upgrading) using liquid fuels as benchmarks. For the CC configurations, the bottoming cycle provides approximately 33% of the gross power but contributes 1.5 times more capital costs than the gas turbine. Hence, the RGT configuration without chemical upgrading has around 30% lower capital costs in exchange for about 7%-points lower efficiency (see Figure 6). However, most of this capital cost benefit is canceled out at a capacity factor of 40% because the lower plant efficiency requires larger pipelines and storage volumes to ensure fuel supply for a given power generation capacity. These results highlight that there is an economic case for implementing decomposition reactors as opposed to direct combustion of liquid fuels.

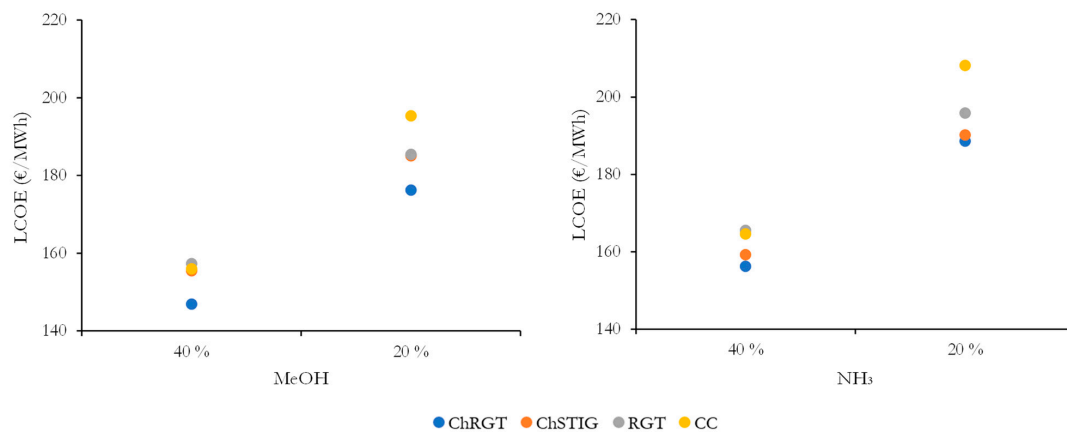


Figure 12. LCOE for MeOH and NH₃ power cycles at different capacity factors.

The levelized cost of electricity (LCOE) for all cases (liquid fuels with chemical upgrading and gaseous fuels) is presented in Figure 13, showing a relatively close trade-off between different factors. The high capital costs of the gaseous fuel plants caused by the infrastructure needed to secure fuel supply (see Table 3) significantly increase the costs of electricity for NG and H₂, whereas the high costs of the liquid fuels (see Figure 5) cancel out the benefit of their relatively low capital costs. In addition, the carbonaceous fuels (NG and MeOH) involve considerable CO₂ emissions that increase the LCOE at the assumed CO₂ tax of 100 EUR/ton. Despite the CO₂ tax, the NG-fired power plants return the lowest costs under the assumptions employed in Table 4, with the ChSTIG and ChRGT configurations returning very similar LCOE numbers for NH₃ and the ChRGT being somewhat advantaged (5.5% cheaper than the ChSTIG) for MeOH.

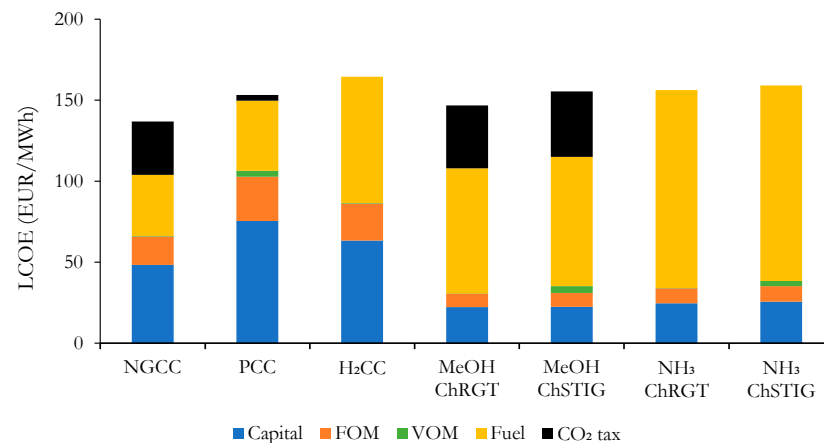


Figure 13. LCOE for the power plants using Sc2 for NG and H₂ and Sc1 for MeOH and NH₃ at a 40% CF and 100 EUR/ton CO₂ tax.

3.4. Sensitivity Analysis

The results of the analysis of sensitivity to process and economic metrics are presented in Figure 14. The key takeaway is that the unabated natural gas combined cycle will remain the most competitive option over a considerable range of variation around the central assumptions given in Table 4 as long as cavern storage is available. However, when the capacity factor drops below approximately 32%, the MeOH ChRGT scheme becomes competitive due to the much lower capital costs required to secure fuel supply (Table 3). When comparing the carbon-free fuels, NH₃ ChRGT can already compete with H₂CC at a capacity factor of 47% due to high H₂ transmission and storage costs. Post-combustion CO₂ capture is not an attractive option for operation at low capacity factors due to the added capital costs of the CO₂ capture, compression, transport and storage infrastructure. Regarding the costs of decarbonization, H₂ only becomes competitive with NG at a CO₂ price of around 200 EUR/ton, whereas NH₃ reaches parity with MeOH at approximately 140 EUR/ton. This difference arises primarily because the relative influence of fuel transmission and storage is considerably larger between NG and H₂ than it is between MeOH and NH₃. When considering the cost of capital (discount rate), gaseous-fueled combined cycles prove most sensitive to this economic parameter due to the higher capital costs resulting from both power plant and transmission and storage systems. With regard to the distance and storage requirements, liquid fuels are relatively insensitive compared to gaseous energy vectors. However, for increases in the cost of primary energy, the schemes with synthesized fuels are more influenced given the thermal conversion efficiency losses from manufacturing these fuels.

Finally, it is highlighted that relative cost reductions achieved in the synthesis processes resulting in a decreased fuel premium for liquid fuels and H₂ can significantly increase the viability as energy carriers for subsequent power generation. For perspective, if cost reductions in the synthesis of fuels were realized through advanced plant designs presented in prior work for MeOH [20] and NH₃ [21], the corresponding fuel premium would be 80.7% and 79.7% respectively, relative to the base costs assumed in this study (given that fuel premium for NH₃ is larger, it represents a higher cost reduction in absolute terms for this fuel). If these technological breakthroughs were achieved, the ChRGT cycles with MeOH and NH₃ would be practically on par with the NGCC case for a CF of 40%, while the liquid fuels would be preferred to H₂ in the whole range of CFs covered in Figure 14. Under this scenario, NH₃ would approximately present an equivalent cost to MeOH for a base CO₂ tax of 100 EUR/ton.

Figure 15 shows the implications for the gaseous fuel plants when cheap cavern storage is not available for the CC configurations. Only at very low storage periods will tank storage for NG be preferable to caverns, whereas H₂ tanks are only justified for less than 1 day of storage. Compared to MeOH, NG and H₂ become more expensive for storage volumes of 2 days and 1 day, respectively. Such low storage volumes are not sufficient to enable the high supply security demanded of these power plants that must sustain the grid during periods with little wind and sun, so liquid fuels should be preferred when salt cavern storage is not available. However, natural gas can also be liquified below −162 °C for lower-cost energy storage in the absence of suitable cavern storage facilities, although the process is much costlier and more energy-intensive than the liquefaction of ammonia at −33 °C.

Despite the general attractiveness of NG when salt caverns are available, plausible scenarios involving low-CF operation in cases requiring longer pipeline distances or larger storage volumes can be envisioned where liquid fuels are clearly superior to gaseous fuels, even when cavern storage is available. Figure 16 illustrates the combinations of transmission and storage requirements where such a transition occurs at two capacity factors.

For the 40% CF case, switching from NG to MeOH or from H₂ to NH₃ requires long transmission distances and large storage volumes. When the available cavern storage site is far away (requiring a large cavern/tank pipeline ratio), however, the breakeven distance to the fuel source shortens considerably. For example, when the pipeline length needed to

connect to the cavern in Sc2 is $3\times$ that of Sc1, the breakeven distance from the fuel source is about 500 km, further shortening as the required storage volume is increased. Storage volume has a considerably stronger influence in the competition between H_2 and NH_3 than in the competition between NG and MeOH because of the high storage costs of H_2 . The crossing between the blue line (tank storage of the gaseous fuel) and the black lines (cavern storage at different cavern/tank pipeline ratios) also indicates how Sc1 becomes more competitive against Sc2 as the distance to the cavern storage site increases.

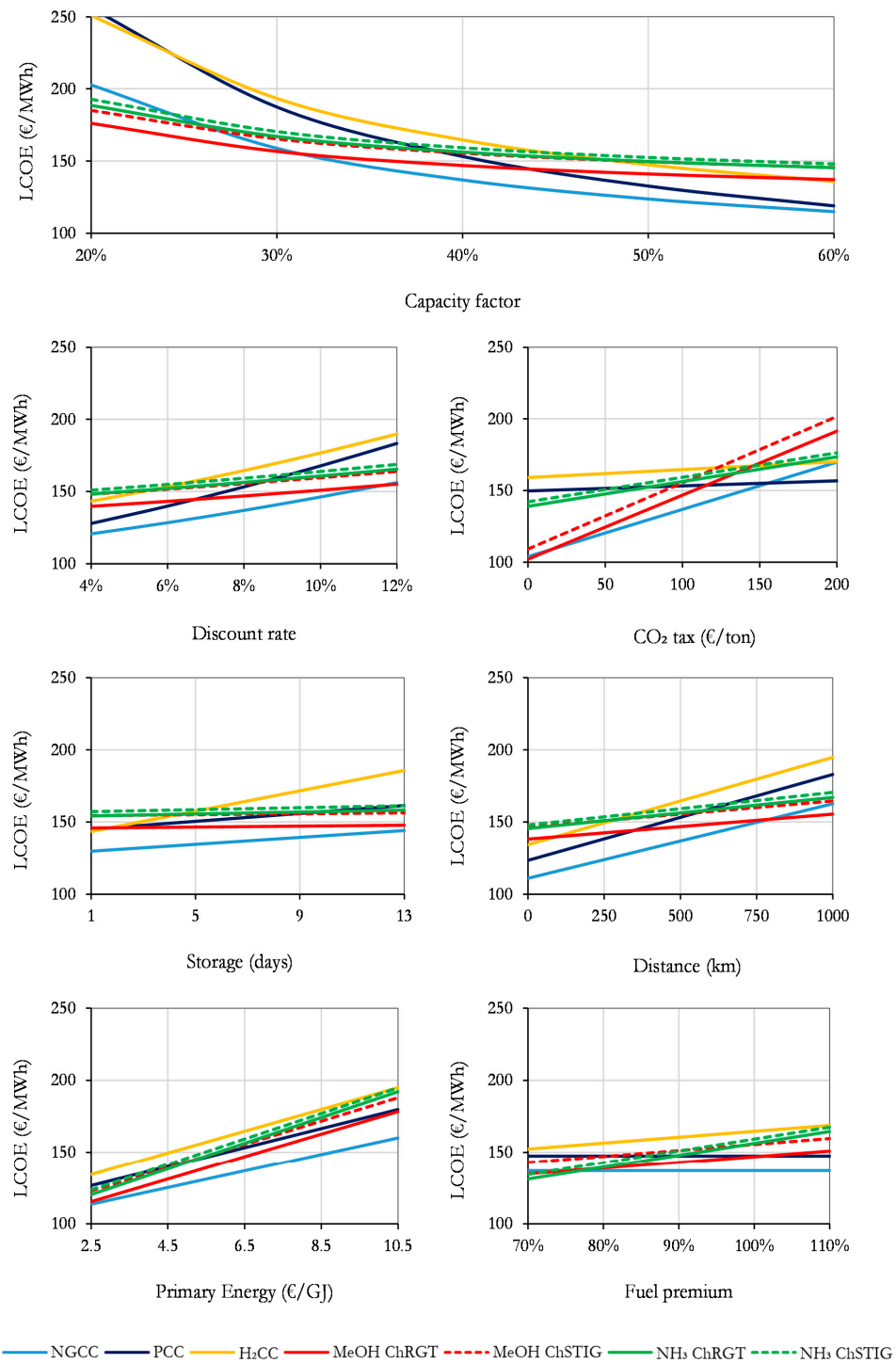


Figure 14. Sensitivity analysis results using Sc2 for NG and H₂ and Sc1 for MeOH and NH₃ with the central assumptions given in Table 4.

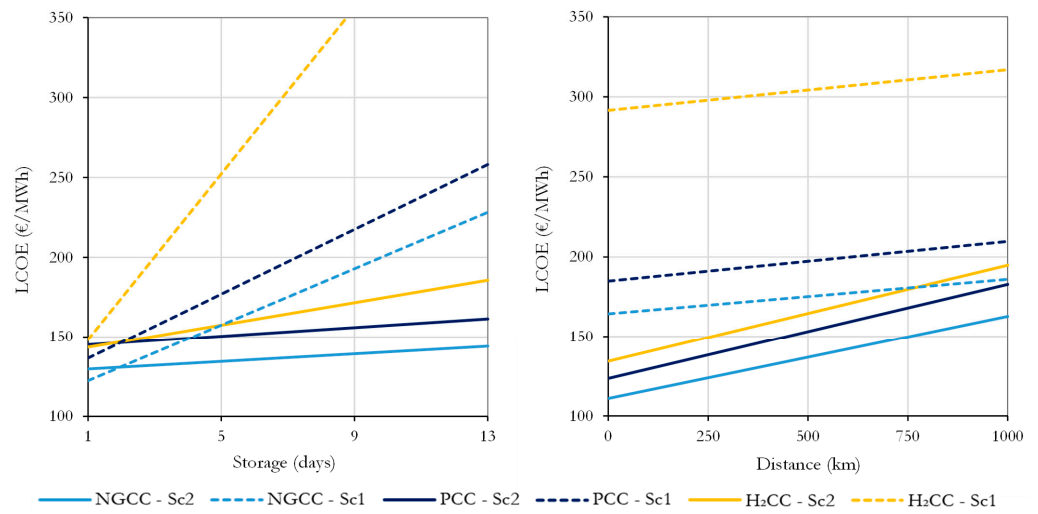


Figure 15. Sc1 vs. Sc2 for gaseous fuel CC in terms of storage days and transmission distance.

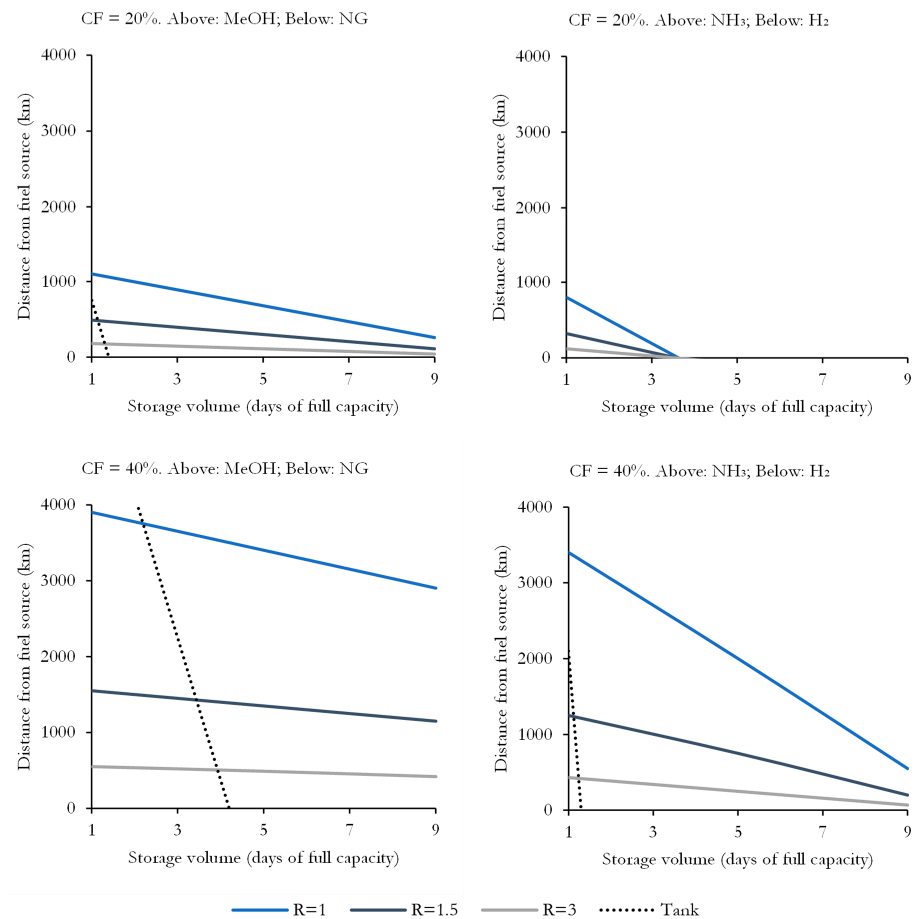


Figure 16. Power cycle and fuel preference map for different transmission distances and storage volumes (areas above the lines favor liquid fuels). Gaseous fuels are represented in Sc2 with three cavern/tank pipeline ratios ($R = 1, 1.5$ and 3) and for Sc1 (Tank).

Liquid fuels become much more attractive when the CF is reduced to 20%. In this event, NH₃ outcompetes H₂ for almost any reasonable transmission and storage scenario that would result in a secure fuel supply. Beyond 4 days of required storage volume, NH₃ is preferred even if the plant is located at the fuel source because NH₃ tank storage is considerably cheaper than H₂ cavern storage (see Table 3). MeOH will also outcompete NG in most fuel distribution scenarios when the plant capacity factor is reduced to 20%,

although the case for the liquid fuel is not quite as strong as in the competition between NH_3 and H_2 .

It can also be mentioned that true energy security may require storage volumes well over 9 days (the upper bound in Figure 16). In any scenario where the availability of the fuel source cannot be fully trusted, liquid fuels will become considerably more attractive because it remains affordable to store a supply of several months.

4. Conclusions

Thermal power plants have an important role to play in future energy systems with high shares of variable renewable energy. This scenario demands flexible power cycles operating at low capacity factors to ensure reliable electricity supply during extended periods with limited availability of wind and sun. Low capital costs are essential to the economics of energy infrastructure with low utilization rates because investment must be recovered over a low number of operating hours. Gas-fired power plants satisfy this criterion, but the transmission and storage infrastructure required to ensure secure fuel supply to these plants can lead to substantial additional costs. When fuel transmission and storage costs are considered with the power plant costs, a case arises for the use of liquid fuels such as MeOH and (liquified) NH_3 instead of gaseous fuels such as natural gas and H_2 . Liquid fuels are considerably more expensive to produce but much cheaper to store and distribute. Hence, the competitiveness of liquid fuels is strongly dependent on the storage volumes and transmission distances required, which can vary greatly between cases.

The case for liquid fuels is strengthened by the potential of chemically recuperated power cycles utilizing waste heat from the turbine exhaust for catalytic decomposition or reforming of the fuel at relatively low temperatures. These cycles allow efficiencies approaching combined cycle performance without a costly bottoming cycle, thus preserving the low capital costs required for cost-effective operation at low utilization rates. Results showed that configurations employing intercooled compression and recuperation economically outperform configurations with steam injection, particularly for methanol, due to the higher endothermicity of the decomposition reaction relative to reforming.

This study shows that advanced MeOH-fueled power cycles can outcompete conventional natural-gas-fired combined cycles at capacity factors below 32%, for a baseline CO_2 price of 100 EUR/ton, a transmission distance of 500 km and salt cavern storage available for the gaseous fuel. The MeOH power plant beats natural gas in economic performance for any transmission distance from caverns above 800 km (baseline capacity factor of 40%). When considering decarbonization, a relatively high CO_2 price exceeding 140 EUR/ton is needed to justify a switch from MeOH to NH_3 , while decarbonization via post-combustion CO_2 capture or H_2 fuel quickly becomes more expensive than NH_3 at low capacity factors due to the high capital requirements for CO_2 capture, transport and storage or H_2 transport and storage.

In conclusion, the merits of liquid fuels such as MeOH and NH_3 should be carefully considered for planning future electricity systems for regions with abundant variable renewable sources where thermal power plants must operate at capacity factors below 50%. Liquid fuels become particularly attractive if the energy security of multi-week fuel storage is highly valued, especially in the absence of a nearby underground formation suitable for gaseous fuel storage. Further studies should focus on evaluating the potential of the proposed power cycles when market prices for fuels like MeOH and NH_3 are considered together with electricity market conditions and available infrastructure in specific locations.

Author Contributions: Conceptualization, S.C. and C.A.d.P.; methodology, S.C. and C.A.d.P.; software, C.A.d.P., J.A.G.d.P.M.d.H. and Á.J.Á.; validation, S.C., J.A.G.d.P.M.d.H. and C.A.d.P.; formal analysis, C.A.d.P., S.C., J.A.G.d.P.M.d.H. and Á.J.Á.; investigation, C.A.d.P., S.C. and J.A.G.d.P.M.d.H.; writing—original draft preparation, C.A.d.P., S.C.; writing—review and editing, C.A.d.P., S.C. and Á.J.Á.; visualization, Á.J.Á. and C.A.d.P.; supervision, Á.J.Á. All authors have read and agreed to the published version of the manuscript.

Funding: This research received funding from the European Union, NextGenerationEU, Ministerio de Universidades Grant RD 289/2021 (UP2021-035).



Data Availability Statement: The complete economic assessment Excel files are available at the following address: <https://bit.ly/ChemRecPower>.

Acknowledgments: The authors would like to acknowledge Honeywell for the free academic license of Unisim Design R481.

Conflicts of Interest: The authors declare no conflict of interest.

Abbreviations

Acronyms

NG	Natural gas
Sc	Scenario
TOC	Total overnight cost
TOT	Turbine outlet temperature
ACF	Annualized cash flows
ASME	American Society of Mechanical Engineers
BEC	Bare erected cost
CCS	Carbon capture and storage
CC	Combined cycle
CF	Capacity factor
Ch	Chemical
COT	Combustor outlet temperature
EPC	Engineering, procurement and construction
Eva	Evaporator
Eco	Economizer
FOM	Fixed operating and maintenance costs
GHG	Greenhouse gas
HAT	Humid air turbine
HP	High pressure
HRSG	Heat recovery steam generator
IP	Intermediate pressure
LP	Low pressure
LCOE	Levelized cost of electricity
LHV	Lower heating value
MEA	Methyl-ethanol amine
MITA	Minimal internal temperature approach
NPV	Net present value
OC	Owners costs
PC	Process contingency
PT	Project contingency
RES	Renewable energy sources
RGT	Recuperated gas turbine
Rh	Reheater
Sh	Superheater
STIG	Steam injection cycle
SEA	Standardized economic assessment
TIT	Turbine inlet temperature
TOT	Turbine outlet temperature
TOC	Total overnight cost
T&S	Transport and storage
tpd	Tons per day
VOM	Variable operating and maintenance cost

List of Symbols

B	Exergy (J)
\dot{E}_{CO_2}	Specific emissions (kg/MWh)
e	Exergy flow (J/mol)
I	Exergy destruction (J)
\dot{m}	Mass flow (kg/s)
P	Pressure (bar)
t	Time (s)
T	Temperature (K)
V	Volume (m ³)
Q	Heat (J)
W	Work (J)
ζ	Exergy efficiency
η	Thermal efficiency (%)

References

- International Energy Agency. *World Energy Outlook*; IEA: Paris, France, 2022.
- National Renewable Energy Lab (NREL). *Flexibility in 21st Century Power Systems*; National Renewable Energy Lab: Golden, CO, USA, 2014.
- Nazir, H.; Muthuswamy, N.; Louis, C.; Jose, S.; Prakash, J.; Buan, M.E.; Flox, C.; Chavan, S.; Shi, X.; Kauranen, P. Is the H₂ economy realizable in the foreseeable future? Part II: H₂ storage, transportation, and distribution. *Int. J. Hydrog. Energy* **2020**, *45*, 20693–20708. [[CrossRef](#)]
- Loschan, C.; Schwabeneder, D.; Maldet, M.; Lettner, G.; Auer, H. Hydrogen as Short-Term Flexibility and Seasonal Storage in a Sector-Coupled Electricity Market. *Energies* **2023**, *16*, 5333. [[CrossRef](#)]
- Moradi, R.; Groth, K.M. Hydrogen storage and delivery: Review of the state of the art technologies and risk and reliability analysis. *Int. J. Hydrog. Energy* **2019**, *44*, 12254–12269. [[CrossRef](#)]
- Blanco, E.C.; Sánchez, A.; Martín, M.; Vega, P. Methanol and ammonia as emerging green fuels: Evaluation of a new power generation paradigm. *Renew. Sustain. Energy Rev.* **2023**, *175*, 113195. [[CrossRef](#)]
- Valera-Medina, A.; Xiao, H.; Owen-Jones, M.; David, W.I.F.; Bowen, P.J. Ammonia for power. *Prog. Energy Combust. Sci.* **2018**, *69*, 63–102. [[CrossRef](#)]
- Luo, C.; Zhang, N.; Lior, N.; Lin, H. Proposal and analysis of a dual-purpose system integrating a chemically recuperated gas turbine cycle with thermal seawater desalination. *Energy* **2011**, *36*, 3791–3803. [[CrossRef](#)]
- Pashchenko, D.; Mustafin, R.; Karpilov, I. Efficiency of chemically recuperated gas turbine fired with methane: Effect of operating parameters. *Appl. Therm. Eng.* **2022**, *212*, 118578. [[CrossRef](#)]
- Sun, Z.; Sun, Z. Hydrogen generation from methanol reforming for fuel cell applications: A review. *J. Cent. South Univ.* **2020**, *27*, 1074–1103. [[CrossRef](#)]
- Araya, S.S.; Liso, V.; Cui, X.; Li, N.; Zhu, J.; Sahlin, S.L.; Jensen, S.H.; Nielsen, M.P.; Kær, S.K. A Review of The Methanol Economy: The Fuel Cell Route. *Energies* **2020**, *13*, 596.
- Jeerh, G.; Zhang, M.; Tao, S. Recent progress in ammonia fuel cells and their potential applications. *J. Mater. Chem. A* **2021**, *9*, 727–752. [[CrossRef](#)]
- Cesaro, Z.; Ives, M.; Nayak-Luke, R.; Mason, M.; Bañares-Alcántara, R. Ammonia to power: Forecasting the levelized cost of electricity from green ammonia in large-scale power plants. *Appl. Energy* **2021**, *282*, 116009. [[CrossRef](#)]
- Pashchenko, D.; Mustafin, R.; Karpilov, I. Ammonia-fired chemically recuperated gas turbine: Thermodynamic analysis of cycle and recuperation system. *Energy* **2022**, *252*, 124081. [[CrossRef](#)]
- Shen, Y.; Nazir, S.M.; Zhang, K.; Duwig, C. Waste heat recovery optimization in ammonia-based gas turbine applications. *Energy* **2023**, *280*, 128079. [[CrossRef](#)]
- Pashchenko, D. Low-grade heat utilization in the methanol-fired gas turbines through a thermochemical fuel transformation. *Therm. Sci. Eng. Prog.* **2022**, *36*, 101537. [[CrossRef](#)]
- Tola, V.; Lonis, F. Low CO₂ emissions chemically recuperated gas turbines fed by renewable methanol. *Appl. Energy* **2021**, *298*, 117146. [[CrossRef](#)]
- Zhao, H.; Yue, P. Performance analysis of humid air turbine cycle with solar energy for methanol decomposition. *Energy* **2011**, *36*, 2372–2380. [[CrossRef](#)]
- Liu, T.; Liu, Q.; Lei, J.; Sui, J.; Jin, H. Solar-clean fuel distributed energy system with solar thermochemistry and chemical recuperation. *Appl. Energy* **2018**, *225*, 380–391. [[CrossRef](#)]
- Arnaiz del Pozo, C.; Cloete, S.; Jiménez Álvaro, Á. Techno-economic assessment of long-term methanol production from natural gas and renewables. *Energy Convers. Manag.* **2022**, *266*, 115785. [[CrossRef](#)]
- Arnaiz del Pozo, C.; Cloete, S. Techno-economic assessment of blue and green ammonia as energy carriers in a low-carbon future. *Energy Convers. Manag.* **2022**, *255*, 115312. [[CrossRef](#)]

22. Cloete, S.; Arnaiz del Pozo, C.; Jiménez Álvaro, Á. System-friendly process design: Optimizing blue hydrogen production for future energy systems. *Energy* **2022**, *259*, 124954. [CrossRef]
23. Anantharaman, R.; Bolland, O.; Booth, N.; Van Dorst, E.; Sanchez Fernandez, E.; Franco, F.; Macchi, E.; Manzolini, G.; Nikolic, D.; Pfeffer, A.; et al. Cesar Deliverable D2.4.3. European Best Practice Guidelines for Assessment of CO₂ Capture Technologies. 2018. Available online: <https://zenodo.org/record/1312801> (accessed on 5 October 2023).
24. Khan, M.N.; Cloete, S.; Amini, S. Efficiency Improvement of Chemical Looping Combustion Combined Cycle Power Plants. *Energy Technol.* **2019**, *7*, 1900567. [CrossRef]
25. Romano, M.C.; Chiesa, P.; Lozza, G. Pre-combustion CO₂ capture from natural gas power plants, with ATR and MDEA processes. *Int. J. Greenh. Gas Control.* **2010**, *4*, 785–797. [CrossRef]
26. Chiesa, P.; Macchi, E. A Thermodynamic Analysis of Different Options to Break 60% Electric Efficiency in Combined Cycle Power Plants. *J. Eng. Gas Turbines Power (Trans. ASME)* **2004**, *126*, 770–785. [CrossRef]
27. Chiesa, P.; Lozza, G.; Mazzocchi, L. Using Hydrogen as Gas Turbine Fuel. *J. Eng. Gas Turbines Power (Trans. ASME)* **2005**, *127*, 73–80. [CrossRef]
28. Arnaiz del Pozo, C.; Cloete, S.; Chiesa, P.; Jiménez Álvaro, Á.; Amini, S. Integration of gas switching combustion and membrane reactors for exceeding 50% efficiency in flexible IGCC plants with near-zero CO₂ emissions. *Energy Convers. Manag. X* **2020**, *7*, 100050. [CrossRef]
29. Jonsson, M.; Bolland, O.; Bücker, D.; Rost, M. Gas turbine cooling model for evaluation of novel cycles. In Proceedings of the ECOS 2005, Trondheim, Norway, 20–22 June 2005.
30. Zhang, F.; Shi, Y.; Yang, L.; Du, X. Kinetics for hydrogen production by methanol steam reforming in fluidized bed reactor. *Sci. Bull.* **2016**, *61*, 401–405. [CrossRef]
31. Kishimoto, M.; Furukawa, N.; Kume, T.; Iwai, H.; Yoshida, H. Formulation of ammonia decomposition rate in Ni-YSZ anode of solid oxide fuel cells. *Int. J. Hydrog. Energy* **2017**, *42*, 2370–2380. [CrossRef]
32. Gazzani, M.; Chiesa, P.; Martelli, E.; Sigali, S.; Brunetti, I. Using Hydrogen as Gas Turbine Fuel: Premixed Versus Diffusive Flame Combustors. *J. Eng. Gas Turbines Power Trans. ASME* **2014**, *136*, 051504. [CrossRef]
33. Cecere, D.; Giacomazzi, E.; Di Nardo, A.; Calchetti, G. Gas Turbine Combustion Technologies for Hydrogen Blends. *Energies* **2023**, *16*, 6829. [CrossRef]
34. Arnaiz del Pozo, C.; Jiménez Álvaro, Á.; Rodríguez Martín, J.; López Paniagua, I.; Sánchez Orgaz, S.; González Fernández, C.; Nieto Carlier, R. Exergy Calculation Modelling Tool for Mixtures in Power Generation: Application to WGS and ASU units of an IGCC Power Plant with Pre-combustion CO₂ Capture. In Proceedings of the XI Congreso Nacional y II Internacional de Ingeniería Termodinámica (11-CNIT), Albacete, Spain, 12–28 June 2019.
35. DeSantis, D.; James, B.D.; Houchins, C.; Saur, G.; Lyubovsky, M. Cost of long-distance energy transmission by different carriers. *iScience* **2021**, *24*, 103495. [CrossRef]
36. Walker, I.; Madden, B.; Tahir, F. *Hydrogen Supply Chain Evidence Base*; Elemental Energy: Cambridge, UK, 2018.
37. Ahluwalia, R.K.; Hua, T.Q.; Peng, J.K.; Kumar, R. System level analysis of hydrogen storage options. In Proceedings of the 2019 Annual Merit Review and Peer Evaluation Meeting, Washington, DC, USA, 29 April–1 May 2019.
38. Nayak-Luke, R.M.; Forbes, C.; Cesaro, Z.; Bañares-Alcántara, R.; Rouwenhorst, K.H.R. Techno-economic aspects of production, storage and distribution of ammonia. In *Techno-Economic Challenges of Green Ammonia as Energy Vector*; Bañares-Alcántara, R., Valera-Medina, A., Eds.; Academic Press: Cambridge, MA, USA, 2020; pp. 191–208.
39. Arnaiz del Pozo, C.; Cloete, S.; Jiménez Álvaro, Á. Standard Economic Assessment (SEA) Tool. Available online: <https://bit.ly/3hyF1TT> (accessed on 5 October 2023).
40. Arnaiz del Pozo, C.; Jiménez Álvaro, Á.; Cloete, S.; García del Pozo Martín de Hijas, J.A. Fuels to Power: ChRGT SEA Files. 2023. Available online: <https://bit.ly/ChemRecPower> (accessed on 5 October 2023).
41. IEAGHG. *The Costs of CO₂ Transport: Post-Demonstration CCS in the EU*; European Technology Platform for Zero Emission Fossil Fuel Power Plants: Brussels, Belgium, 2011.
42. IEAGHG. *The Costs of CO₂ Storage: Post-Demonstration CCS in the EU*; European Technology Platform for Zero Emission Fossil Fuel Power Plants: Brussels, Belgium, 2011.
43. Cloete, S.; García del Pozo Martínez de Hijas, J.A.; Arnaiz del Pozo, C.; Jiménez Álvaro, A. *Future Fuels for Gas-Fired Power Production. A Comparative Techno-Economic Assessment*; Technical Report; Universidad Politécnica de Madrid: Madrid, Spain; SINTEF Industry: Trondheim, Norway, 2023. [CrossRef]

Disclaimer/Publisher’s Note: The statements, opinions and data contained in all publications are solely those of the individual author(s) and contributor(s) and not of MDPI and/or the editor(s). MDPI and/or the editor(s) disclaim responsibility for any injury to people or property resulting from any ideas, methods, instructions or products referred to in the content.